



ELSEVIER

Available online at [www.sciencedirect.com](http://www.sciencedirect.com)

SCIENCE @ DIRECT®

Physics Letters B 549 (2002) 48–57

---

---

PHYSICS LETTERS B

---

---

[www.elsevier.com/locate/npe](http://www.elsevier.com/locate/npe)

# Determination of the semi-leptonic branching fraction of charm hadrons produced in neutrino charged-current interactions

CHORUS Collaboration

A. Kayis-Topaksu, G. Onengüt

*Çukurova University, Adana, Turkey*

M. de Jong, O. Melzer, R.G.C. Oldeman<sup>1</sup>, E. Pesen, F.R. Spada<sup>2</sup>, R. van Dantzig,  
J.L. Visschers

*NIKHEF, Amsterdam, The Netherlands*

M. Güler<sup>3</sup>, M. Serin-Zeyrek, R. Sever, P. Tolun, M.T. Zeyrek

*METU, Ankara, Turkey*

N. Armenise, M.G. Catanesi, M. De Serio, M. Ieva, M.T. Muciaccia, E. Radicioni,  
S. Simone

*Università di Bari and INFN, Bari, Italy*

A. Bülte, K. Winter

*Humboldt Universität, Berlin, Germany<sup>4</sup>*

R. El-Aidi, B. Van de Vyver<sup>5,6</sup>, P. Vilain<sup>7</sup>, G. Wilquet<sup>7</sup>

*Inter-University Institute for High Energies (ULB-VUB), Brussels, Belgium*

B. Saitta

*Università di Cagliari and INFN, Cagliari, Italy*

E. Di Capua

*Università di Ferrara and INFN, Ferrara, Italy*

S. Ogawa, H. Shibuya

*Toho University, Funabashi, Japan*

A. Artamonov<sup>8</sup>, M. Chizhov<sup>9</sup>, M. Doucet<sup>10</sup>, I.R. Hristova<sup>9</sup>, T. Kawamura, D. Kolev<sup>9</sup>,  
H. Meinhard, J. Panman, I.M. Papadopoulos, S. Ricciardi<sup>11</sup>, A. Rozanov<sup>12</sup>,  
R. Tsenov<sup>9</sup>, J.W.E. Uiterwijk, P. Zucchelli<sup>13</sup>

*CERN, Geneva, Switzerland*

**J. Goldberg**

*Technion, Haifa, Israel*

**M. Chikawa**

*Kinki University, Higashiosaka, Japan*

**E. Arik**

*Bogazici University, Istanbul, Turkey*

**J.S. Song, C.S. Yoon**

*Gyeongsang National University, Jinju, South Korea*

**K. Kodama, N. Ushida**

*Aichi University of Education, Kariya, Japan*

**S. Aoki, T. Hara**

*Kobe University, Kobe, Japan*

**T. Delbar, D. Favart, G. Grégoire, S. Kalinin, I. Maklioueva**

*Université Catholique de Louvain, Louvain-la-Neuve, Belgium*

**P. Gorbunov<sup>6</sup>, V. Khovansky, V. Shamanov, I. Tsukerman**

*Institute for Theoretical and Experimental Physics, Moscow, Russian Federation*

**N. Bruski, D. Frekers**

*Westfälische Wilhelms-Universität, Münster, Germany<sup>4</sup>*

**K. Hoshino, M. Komatsu, M. Miyanishi, M. Nakamura, T. Nakano, K. Narita, K. Niu,  
K. Niwa, N. Nonaka, O. Sato, T. Toshito**

*Nagoya University, Nagoya, Japan*

**S. Buontempo, A.G. Cocco, N. D’Ambrosio, G. De Lellis, F. Di Capua, G. De Rosa,  
A. Ereditato, G. Fiorillo, M. Messina, P. Migliozzi, C. Pistillo, L. Scotto Lavina,  
P. Strolin, V. Tioukov**

*Università Federico II and INFN, Naples, Italy*

K. Nakamura, T. Okusawa

*Osaka City University, Osaka, Japan*

U. Dore, P.F. Loverre, L. Ludovici, P. Righini, G. Rosa, R. Santacesaria, A. Satta

*Università La Sapienza and INFN, Rome, Italy*

E. Barbuto, C. Bozza, G. Grella, G. Romano, C. Sirignano, S. Sorrentino

*Università di Salerno and INFN, Salerno, Italy*

Y. Sato, I. Tezuka

*Utsunomiya University, Utsunomiya, Japan*

Received 8 October 2002; accepted 16 October 2002

Editor: L. Montanet

## Abstract

During the years 1994–1997, the emulsion target of the CHORUS detector was exposed to the CERN-SPS Wide Band Neutrino Beam. The improvements of the past few years in the automatic emulsion scanning systems allowed a sample of events located in emulsion to be used for studies of charm production. Based on a sample of 56 172  $\nu_\mu$  charged-current interactions analysed so far, we find a value of  $B_\mu = 0.093 \pm 0.009(\text{stat.}) \pm 0.009(\text{syst.})$  for the semi-leptonic branching fraction of charm hadrons. The result for events with visible energy larger than 30 GeV,  $B_\mu = 0.102 \pm 0.016(\text{stat.}) \pm 0.010(\text{syst.})$ , can be combined with the existing measurements of the dimuon rate to yield a value of  $0.219 \pm 0.022$  for the magnitude of the Cabibbo–Kobayashi–Maskawa matrix element  $|V_{cd}|$ .

© 2002 Elsevier Science B.V. All rights reserved.

## 1. Introduction

Charm production in neutrino charged-current interactions has been studied in several experiments, in particular, CDHS [1], CCFR [2], CHARM [3], CHARM-II [4], NOMAD [5] and NuTeV [6] by means of electronic detectors and through the analysis of dimuon events. In these events, the leading muon is interpreted as originating from the neutrino vertex and the other, of opposite charge, as the product of the charmed particle semi-leptonic decay. The study of dimuon events provides information on the strange quark content of the nucleon, the charm mass, and the Cabibbo–Kobayashi–Maskawa (CKM) matrix elements  $|V_{cd}|$  and  $|V_{cs}|$ . Experiments of this type, however, suffer from significant background ( $\sim 30\%$ ) in which the second muon originates from an undetected decay in flight of a pion or a kaon rather than from

<sup>1</sup> Now at University of Pennsylvania, Philadelphia, USA.

<sup>2</sup> And INFN, Rome, Italy.

<sup>3</sup> Now at Nagoya University, Nagoya, Japan.

<sup>4</sup> Supported by the German Bundesministerium für Bildung und Forschung under contract numbers 05 6BU11P and 05 7MS12P.

<sup>5</sup> Fonds voor Wetenschappelijk Onderzoek, Belgium.

<sup>6</sup> Now at CERN, 1211 Geneva 23, Switzerland.

<sup>7</sup> Fonds National de la Recherche Scientifique, Belgium.

<sup>8</sup> On leave of absence from ITEP, Moscow.

<sup>9</sup> On leave of absence from St. Kliment Ohridski University of Sofia, Bulgaria.

<sup>10</sup> Now at University of Maryland, MD, USA.

<sup>11</sup> Now at Royal Holloway College, University of London, Egham, UK.

<sup>12</sup> Now at CPPM CNRS-IN2P3, Marseille, France.

<sup>13</sup> On leave of absence from INFN, Ferrara, Italy.

a charm decay. Moreover, the type of charmed particle and its decay topology cannot be identified in these experiments. The overall normalization of the charm production rate in terms of the dimuon rate is given by the average semi-leptonic branching fraction, defined as the weighted average of the semi-leptonic branching fraction for individual charmed hadron species with the corresponding fragmentation fractions as weights.

Compared to the study of dimuon events, a much lower level of background can be achieved using an emulsion target which provides a sub-micron spatial resolution and, hence, the topological identification of charmed hadron decays. This technique has been applied in the E531 experiment at FNAL to measure the fragmentation fractions  $f_{D_i}$  [7]. These data have been combined [2,8,9] with the individual semi-leptonic branching fractions to yield  $B_\mu = 0.099 \pm 0.012$ , the value used by the Particle Data Group [10] in determining the magnitude of the CKM matrix element  $|V_{cd}|$ . However, the statistics accumulated in the E531 experiment was limited to 125 charm events.

Only recently, with the development of automatic scanning devices of much higher speed within CHORUS, has it become possible to study large samples of charm events produced in nuclear emulsion [11]. The present result is based on a sample of  $956 \pm 35$  charm events, after correcting for the purity of the selection procedure. The number of events is sufficient to determine the average semi-leptonic branching fraction directly from the number of charm events with a secondary muon in the final state, with an error comparable to the existing indirect measurements.

## 2. The experimental apparatus

The CHORUS detector [12] is a hybrid set-up that combines a nuclear emulsion target with various electronic detectors. The nuclear emulsion acts both as target for neutrino interactions and as detector, allowing three-dimensional reconstruction of short-lived particles such as the tau lepton and charmed hadrons. The emulsion target has a total mass of 770 kg and is segmented into four stacks, each consisting of eight modules, in turn composed of 36 plates with a size of  $36 \times 72 \text{ cm}^2$ . Each plate has a  $90 \text{ }\mu\text{m}$  plastic support coated on both sides with a

$350 \text{ }\mu\text{m}$  emulsion layer [13]. Each stack is followed by three interface emulsion sheets with a  $90 \text{ }\mu\text{m}$  emulsion layer on both sides of an  $800 \text{ }\mu\text{m}$  thick plastic base and by a set of scintillating fibre tracker planes. The interface sheets and the fibre trackers provide accurate predictions of particle trajectories into the emulsion stack for the location of the vertex positions. The accuracy of the fibre tracker prediction is about  $150 \text{ }\mu\text{m}$  in position and  $2 \text{ mrad}$  in the track angle.

The emulsion scanning has been performed by fully automatic microscopes equipped with CCD cameras and a read-out system [14]. The track finding efficiency is higher than 98% for track slopes less than  $400 \text{ mrad}$  with respect to the direction perpendicular to the emulsion plates.

The electronic detectors downstream of the emulsion target include a hadron spectrometer which measures the bending of charged particles in an air-core magnet, a calorimeter where the energy and direction of showers are measured and a muon spectrometer which determines the charge and momentum of muons.

## 3. Data collection

The West Area Neutrino Facility (WANF) at CERN provides a beam of  $27 \text{ GeV}$  average energy consisting mainly of  $\nu_\mu$  with a 5%  $\bar{\nu}_\mu$  contamination. For the four years in which the emulsion target was exposed, the integrated beam intensity corresponds to  $5.06 \times 10^{19}$  protons on target. The analysis of the data from the electronic detectors allows the identification of the set of events possibly originating from the emulsion stacks.

The CHORUS experiment was designed primarily to search for  $\nu_\mu \rightarrow \nu_\tau$  oscillation. For the first phase of the analysis, the events were subdivided in two classes, the one-muon and zero-muon samples, and the data selection and vertex location procedures were optimized for the detection of tau leptons decaying into a muon or into a single charged hadron, respectively. The one-muon sample consists largely of  $\nu_\mu$  charged-current interactions and serves as a suitable starting point for the analysis of charm production in neutrino charged-current interactions. For the vertex location, the muon track reconstructed by the electronic detectors is searched for in the interface sheets, and then

followed from one plate to the next using the segments in the most upstream 100  $\mu\text{m}$  of each plate. Once it is no longer found in two consecutive plates, the first of these is defined as the *vertex plate*. This plate may contain the primary or the decay vertex, or both.

The charm decay search is performed using the *netscan* method, originally developed for the DONUT experiment [15]. It consists in recording all track segments within a given angular acceptance in a volume surrounding the assumed vertex position. In CHORUS, the angular acceptance is 400 mrad and the size of the volume is  $1.5 \times 1.5 \text{ mm}^2$  transversely and 6.3 mm longitudinally. The latter corresponds to eight plates: one plate upstream from the vertex plate acting as a veto for passing tracks, the vertex plate itself, and six plates downstream. The parameters of all track segments found in this volume are stored in a database. Typically, five thousand track segments are recorded per event. With the scanning systems used, the treatment of one event takes about 11 min on a single microscope. The results presented here are based on a sample of 56 172 events analysed with this method, out of the 143 742 one-muon events that have so far been located.

#### 4. Reconstruction and selection of decay topologies

The offline reconstruction program first aims to select from the large number of recorded track segments only those belonging to the neutrino interaction under study. First, plate-to-plate alignment is performed by comparing the pattern of segments in consecutive plates. After connection of all matched segments, the alignment is repeated to reach a residual of less than 0.5  $\mu\text{m}$  for the segment positions with respect to the fitted tracks. The majority of the tracks are due to low-energy particles, discarded on the basis of goodness-of-fit for a straight line hypothesis. Another source of background are the tracks passing through the volume. After removing these as well, the mean number of tracks to be further analysed is about 40. A more detailed description of the alignment and track finding algorithms is given in Ref. [16].

After this initial selection of potentially interesting track segments, any further reconstruction can be formulated as a problem of error propagation thanks to

the detailed understanding of the measurement errors for individual segments. First, the segments are combined to form tracks, taking into account the effect of multiple Coulomb scattering. This yields a set of correctly normalized errors on the track parameters, and provides a  $\chi^2$  probability criterion to remove outlier segments. In turn, the tracks are associated to vertices, again using a  $\chi^2$  probability criterion to decide which tracks intersect. As the emulsion integrates the tracks of all particles that pass at any time in the two year long exposure, only the electronic detectors can validate that a given track belongs to the event under study. The connection between emulsion tracks and tracks in the electronic detectors is based on their angular difference, again employing a  $\chi^2$  probability criterion. Finally, events in which at least two tracks are matched to electronic detector tracks but not associated to the same vertex are selected as candidate charm events. The reconstruction and selection algorithms are described in detail in Ref. [17].

In total, 1055 events are selected. To evaluate the purity of the selection algorithms, a subsample of 244 selected events was visually inspected. The purpose of the eye-scan is twofold: to distinguish genuine secondary vertices from artefacts in the reconstruction and to distinguish secondary decay vertices from hadronic interactions. Out of the 244 events, 11 do not show a secondary vertex, but instead are due to any of the following: non-Gaussian tails in the track parameters preventing primary tracks from being associated to the primary vertex, inefficiencies in the track reconstruction which cause through-going tracks to appear to stop, electron pairs, and secondary vertices on tracks not related to the event. An additional 12 events are identified as secondary hadronic interactions through the presence of nuclear activity at the supposed decay point or through a number of prongs inconsistent with charge conservation. This results in a selection purity of  $0.91 \pm 0.02$ , which brings the corrected number of selected charm events to

$$N^{\text{selected}} = 956 \pm 35. \quad (1)$$

#### 5. Selection efficiency

The efficiency of the charm selection was evaluated with a GEANT3 [18] based simulation of

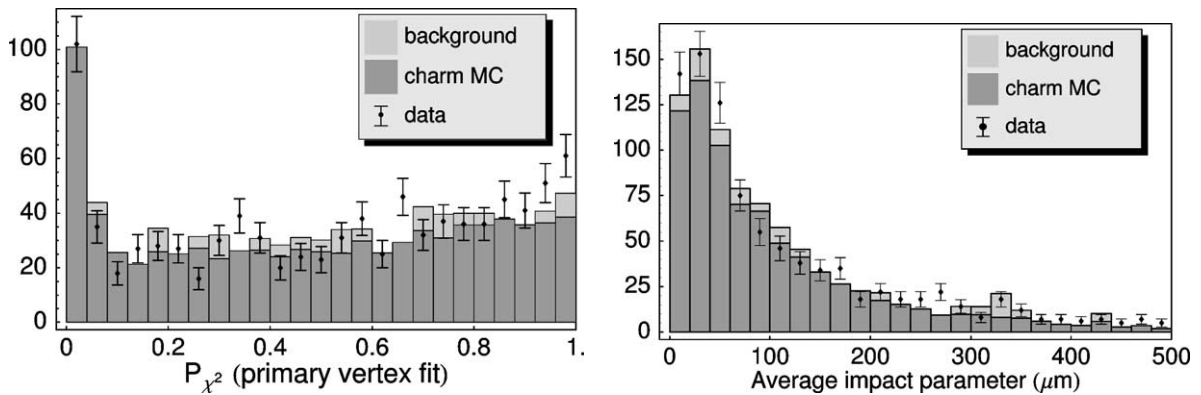


Fig. 1. Left: distribution of the  $\chi^2$  fit probability for the primary vertex in events where there is more than one reconstructed track at the primary. Right: the average impact parameter of secondary tracks to the primary vertex for events where the primary track is not isolated. The samples are described in the text.

the experiment. Large samples of deep-inelastic neutrino interactions were generated according to the beam spectrum using the JETTA [19] generator derived from LEPTO [20] and JETSET [21]. The simulated response of the CHORUS electronic detectors is processed through the same reconstruction program used for the data.

To evaluate the netscan efficiency, realistic conditions of track densities need to be reproduced. This was achieved by merging the emulsion data of the simulated events with real netscan data which do not have a reconstructed vertex but contain tracks which stop or pass through the netscan fiducial volume, representing the real background. The combined data are passed through the same netscan reconstruction and selection programs as used for real data.

Fig. 1 shows a comparison between real data and simulated data for two quantities of particular interest. The data sample are the 1055 selected events, with a purity of  $0.91 \pm 0.02$ . The simulated sample consists of deep-inelastic neutrino interactions in which a charmed particle is produced. After applying the same selection as for the data, the simulated sample is a factor of five larger than the data sample. The background from secondary interactions and reconstruction artefacts has not been explicitly simulated, but was extrapolated from the 23 visually identified background events.

The first distribution in Fig. 1 shows the  $\chi^2$  probability for the vertex fit. Apart from the overall agreement between the data and the simulation, the fact that the distribution is flat except for a relatively modest

peak at low fit probability demonstrates the sound understanding of the measurement errors. The second distribution shows the average impact parameter of secondary tracks to the primary vertex, for the subsample of events where there is more than one primary track reconstructed. Of all geometric quantities, the average impact parameter is the one most closely related to the proper decay length. Again, good agreement is found between data and simulation.

The only quantity of interest for which a discrepancy exists between data and simulation is the reconstructed multiplicity of charged tracks at the secondary vertex. In the data, the ratio of two-prong to one-prong events is  $1.16 \pm 0.08$ , compared to  $1.71 \pm 0.11$  for the simulation, in both cases quoting only the statistical error. At present, this discrepancy is not yet understood but the data suggest shortcomings in the event generator rather than problems with the description of the emulsion response. First, the contribution of quasi-elastic and diffractive processes to charm production relative to the deep-inelastic process is poorly known. Second, the charmed particle branching ratios are affected by considerable uncertainty. Varying the parameters that define the event generator hypotheses within the range allowed by their experimental uncertainty leads to significant changes in the ratio of two-prong to one-prong events, covering the ratio found in the data.

However, it is worth stressing that the effect of this discrepancy on the present analysis is mitigated by the fact that the result on the average semileptonic branching fraction is relatively insensitive to

variations in the event generator. The determination of the average semi-leptonic branching fraction relies on a ratio of efficiencies: the first for the selection of a charmed particle decay, the second for the selection of a charmed particle decaying semi-leptonically. Any uncertainties on the absolute level of the selection efficiencies cancel in the ratio.

Table 1 shows the selection efficiencies for each of the four weakly decaying charmed hadrons, without or with the requirement for the decay to be semi-leptonic. Charmed hadron species other than  $D^+$ ,  $D^0$ ,  $D_s^+$  and  $\Lambda_c$  decay through the electromagnetic or strong interaction to one of these four. The correction factor for the efficiency in the determination of the semi-leptonic branching fraction is defined as

$$R = \frac{\sum_{D_i} \epsilon_{D_i} f_{D_i}}{\sum_{D_i} \epsilon_{D_i^\mu} f_{D_i}}, \quad (2)$$

where  $\epsilon_{D_i}$  is the selection efficiency for charm species  $D_i$ ,  $\epsilon_{D_i^\mu}$  the selection efficiency for semi-leptonic decays of  $D_i$ , and  $f_{D_i}$  the fragmentation fraction.

Table 2 shows the different estimates of the fragmentation fractions used for this analysis. The column labelled JETTA is based on the sample of sim-

ulated events, the error is statistical only. The numbers between parentheses correspond to enhanced contributions of  $D_s$  and  $\Lambda_c$  to approximate the effect of including diffractive and quasi-elastic processes, assuming for each of the two a cross-section equal to 7.5% of the deep-inelastic cross-section [22,23].

The column labelled E531 is the only direct experimental measurement of these quantities, performed by the E531 emulsion experiment but reanalysed by Bolton [8]. Because of the different energy dependence of the deep-inelastic, diffractive, and quasi-elastic charm production processes, the fractions vary as a function of energy. In the present analysis, there is no explicit minimum for the visible energy. Nevertheless, the 4 GeV minimum for the energy measured in the calorimeter translates into an effective minimum visible energy of about 10 GeV once the primary muon energy has been included.

Because of the requirements for the CHORUS neutrino oscillation analysis, the vertex location has in the past been restricted to events where the measured momentum of the primary muon lies below 30 GeV. However, Monte Carlo studies show that the effect on the correction factor  $R$  is only a fraction of a percent, due to cancellations in the ratio.

The value of  $R$  has been evaluated under all acceptable hypotheses for both the selection efficiencies and the fragmentation fractions. The result varies between 0.968 and 1.049. In the absence of any compelling argument in favour of or against any one of the sets of assumptions, we will in the following use the average value

$$R = 1.01 \pm 0.05, \quad (3)$$

with the systematic error estimated from the variation under different hypotheses.

Table 1

The charm selection efficiency, determined from the simulation, for each of the four weakly decaying charmed hadrons which are produced. The third column indicates the selection efficiency for the case where the charmed hadron decays semi-leptonically. The errors are statistical only

Species	Selection efficiency	
	$D_i \rightarrow \text{any}$	$D_i \rightarrow \mu X$
$D^+$	$0.369 \pm 0.010$	$0.41 \pm 0.02$
$D^0$	$0.541 \pm 0.006$	$0.50 \pm 0.02$
$D_s^+$	$0.440 \pm 0.018$	$0.45 \pm 0.06$
$\Lambda_c$	$0.335 \pm 0.015$	$0.29 \pm 0.07$

Table 2

The fragmentation fractions for charm quarks produced in charged-current neutrino interactions after any strong or electromagnetic decays. The different columns are described in the text

Species	JETTA		E531	
			$E_{\text{vis}} > 5 \text{ GeV}$	$E_{\text{vis}} > 20 \text{ GeV}$
$D^+$	$0.225 \pm 0.003$	(0.196)	$0.16 \pm 0.04$	$0.20 \pm 0.05$
$D^0$	$0.612 \pm 0.003$	(0.532)	$0.53 \pm 0.05$	$0.56 \pm 0.05$
$D_s$	$0.072 \pm 0.002$	(0.128)	$0.13 \pm 0.04$	$0.11 \pm 0.04$
$\Lambda_c$	$0.092 \pm 0.002$	(0.145)	$0.17 \pm 0.04$	$0.11 \pm 0.04$

For the sample of simulated events,<sup>14</sup> the fraction of  $D^0$  mesons decaying into neutral particles is 4.2%. A recent analysis [24] indicates that decay modes not accounted for in the past may be responsible for an underestimate of this fraction. As the selection efficiency for neutral decay modes is zero, an increase in this fraction leads to a decrease of the  $D^0 \rightarrow$  any selection efficiency, in turn affecting the correction factor  $R$ . For the extreme case where 20% of  $D^0$  mesons decay into neutral particles, the  $D^0$  selection efficiency would be 45% instead of 54%. Assuming a  $D^0$  fragmentation fraction of 0.612 (0.53), this would reduce  $R$  by a factor of 0.88 (0.89).

## 6. Identification of the secondary muon

Muons are identified in the downstream detectors, the calorimeter and the muon spectrometer. Any charged particle that reaches the muon spectrometer is identified as a muon. The probability for a charged pion or kaon to traverse 5.2 interaction lengths in the calorimeter without interacting is smaller than 5%. However, a sample of muons based exclusively on this requirement would lead to a loss in angular acceptance and to a threshold for the muon momentum between 1.6 GeV/ $c$  and 2.5 GeV/ $c$ , depending on the track angle. The effect is marginal for the primary muon from the neutrino interaction, but becomes particularly severe for secondary muons from charm decay due to their relatively soft spectrum. An attempt is made to identify also muons exiting sideways from the calorimeter or stopping in the calorimeter based on the presence of a minimum ionizing particle in the calorimeter. There exist two independent algorithms for this purpose. The first is based on a neural network analysing the pattern of energy deposits in the scintillators. The second is a track finding algorithm using the information of streamer tube planes inserted between the calorimeter modules. Each of the two algorithms is applied independently for the two projections, leading to a total of four possible tags for muons in the calorimeter. The minimum requirement

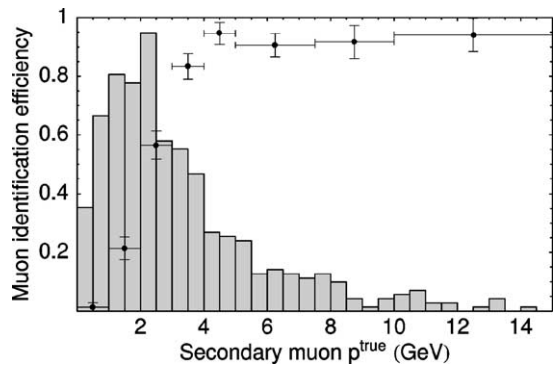


Fig. 2. The efficiency of the muon identification as a function of the true muon momentum, with the histogram indicating the spectrum of secondary muon momenta for the simulated events after charm selection.

for muon identification is a positive result from three out of four.

As shown in Fig. 2, the identification efficiency is of the order of 95% for muon momenta above 4 GeV, the region where all muons reach the muon spectrometer. However, identification of muons in the calorimeter is considerably less efficient, precisely in the region where secondary muons from charm decay are expected. When integrated over the spectrum for simulated charm events, the secondary muon identification has average efficiency and average purity of about 55% and 60%, respectively.

The fact that muons identified in the muon spectrometer can also be identified in the calorimeter has been used to validate the results of the simulation. The systematic error on the efficiency and purity of muon identification has been determined by varying the requirements. Out of the  $956 \pm 35$  selected charm events, the number of events with a secondary muon is

$$N_{2\mu}^{\text{selected}} = 88 \pm 10(\text{stat.}) \pm 8(\text{syst.}), \quad (4)$$

corrected for the efficiency and purity of the muon identification.

## 7. Results and conclusion

The average semi-leptonic branching fraction can be written in terms of measurable quantities as

$$B_{\mu} = \sum_{D_i} f_{D_i} \text{BR}(D_i \rightarrow \mu X) = \frac{N_{2\mu}^{\text{selected}}}{N^{\text{selected}}} \times R, \quad (5)$$

<sup>14</sup> The same sample was used in a previous analysis [11]. However, in that context, the result for the  $D^0$  production cross section referred exclusively to decay modes with charged particles.



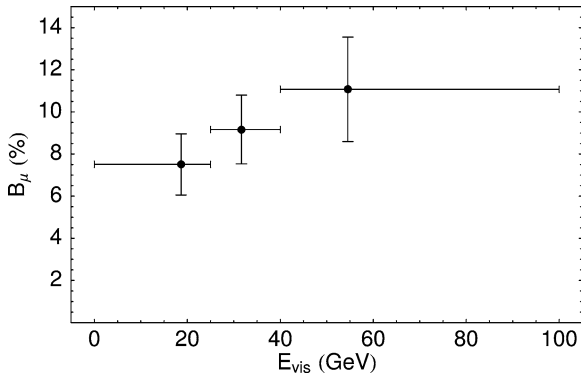


Fig. 3. The average semi-leptonic branching fraction as a function of the visible energy. The horizontal bars indicate the width of the energy bin. The vertical bars are drawn at the mean value of the energy in each bin, and their height indicates the statistical error on  $B_\mu$ .

where  $N^{\text{selected}}$  is the number of selected events, corrected for the selection purity, and  $N_{2\mu}^{\text{selected}}$  is the number of selected events with a secondary muon in the final state, corrected for the selection purity as well as for the muon identification efficiency and purity. Combining Eqs. (1), (3) and (4), we find that

$$B_\mu = 0.093 \pm 0.009(\text{stat.}) \pm 0.009(\text{syst.}), \quad (6)$$

where the systematic error includes the uncertainty on the Monte Carlo description of the muon identification, as well as the uncertainty on the correction factor related to the fragmentation fractions and the selection efficiencies for different species and different topologies. The second gives a minor contribution, and one can likewise expect any other sources of systematic error which have not been explicitly estimated to be negligible compared to the present statistical error and the present uncertainty on the muon identification.

Given the currently available statistics, the energy dependence of  $B_\mu$  can as yet be determined only approximately in the CHORUS experiment. Dividing the events in three samples on the basis of the visible energy and applying Eq. (5) for each subsample leads to the result shown in Fig. 3. The errors shown are only statistical, but these are dominant anyhow as there are only a few dozen selected events with a second muon in each energy bin.

The semi-leptonic branching fraction, as defined in this context, is an empirical parameter, not a fundamental constant. Due to the energy dependence,

the value for  $B_\mu$  measured in one experiment, with a given neutrino beam and a given acceptance as a function of neutrino energy, cannot be applied directly to determine  $|V_{cd}|$  from the measurement of  $B_\mu |V_{cd}|^2$  performed by a different experiment, with a different neutrino beam and a different energy dependence for the acceptance. The CCFR experiment has extracted a value for  $|V_{cd}|$  by combining its study of opposite-sign dimuon events with a determination of  $B_\mu$  based on the E531 data, considering only events with a visible energy above 30 GeV [8,9]. This approach has been adopted by the Particle Data Group (PDG) as well, even though it is then applied on the average over  $B_\mu |V_{cd}|^2$  measurements from different experiments. For the sake of comparison, we have extracted  $B_\mu$  for the subsample of events with visible energy larger than 30 GeV. This yields a value of

$$B_\mu = 0.102 \pm 0.016(\text{stat.}) \pm 0.010(\text{syst.}). \quad (7)$$

Adding the statistical and systematic errors in quadrature, and combining with the average  $B_\mu |V_{cd}|^2$  used by the PDG,

$$B_\mu |V_{cd}|^2 = (0.49 \pm 0.05) \times 10^{-2}, \quad (8)$$

we find that

$$|V_{cd}| = 0.219 \pm 0.022, \quad (9)$$

to be compared with  $|V_{cd}| = 0.224 \pm 0.016$ , the value currently quoted by the PDG and based on the determination of  $B_\mu$  from E531 data. As already noted, the present analysis assumes a value of 4.2% for the fraction of  $D^0$  mesons decaying into neutral particles. A higher value would increase the result quoted in Eq. (9). If unitarity is assumed, the 90% confidence interval for  $|V_{cd}|$  stretches from 0.219 to 0.225.

A second phase of analysis of the CHORUS data is well under way with improved reconstruction codes and scanning systems, and a sample of 3000 charm events will soon be available.

## Acknowledgements

We gratefully acknowledge the help and support of the neutrino-beam staff and of the numerous technical collaborators who contributed to the detector

construction, operation, emulsion pouring, development, and scanning. The experiment has been made possible by grants from the Institut Interuniversitaire des Sciences Nucléaires and the Interuniversitair Instituut voor Kernwetenschappen (Belgium); the Israel Science Foundation (Grant 328/94) and the Technion Vice President Fund for the Promotion of Research (Israel); CERN (Geneva, Switzerland); the German Bundesministerium für Bildung und Forschung (Germany); the Institute of Theoretical and Experimental Physics (Moscow, Russia); the Istituto Nazionale di Fisica Nucleare (Italy); the Promotion and Mutual Aid Corporation for Private Schools of Japan and Japan Society for the Promotion of Science (Japan); the Korea Research Foundation (Grant KRF-2001-005-D00006) (Republic of Korea); the Foundation for Fundamental Research on Matter FOM and the National Scientific Research Organization NWO (The Netherlands); and the Scientific and Technical Research Council of Turkey (Turkey). We gratefully acknowledge their support.

## References

- [1] CDHS Collaboration, H. Abramowicz, et al., *Z. Phys. C* 15 (1982) 19.
- [2] CCFR Collaboration, S.A. Rabinowitz, et al., *Phys. Rev. Lett.* 70 (2) (1993) 134.
- [3] CHARM Collaboration, M. Jonker, et al., *Phys. Lett. B* 107 (1981) 241.
- [4] CHARM-II Collaboration, P. Vilain, et al., *Eur. Phys. J. C* 11 (1999) 19.
- [5] NOMAD Collaboration, P. Astier, et al., *Phys. Lett. B* 486 (2000) 35.
- [6] NuTeV Collaboration, M. Goncharov, et al., *Phys. Rev. D* 64 (2001) 112006.
- [7] E531 Collaboration, N. Ushida, et al., *Phys. Lett. B* 206 (2) (1988) 375.
- [8] T. Bolton, hep-ex/9708014.
- [9] CCFR Collaboration, A.O. Bazarko, et al., *Z. Phys. C* 65 (1995) 189.
- [10] Particle Data Group, D.E. Groom, et al., *Eur. Phys. J. C* 15 (2000) 1.
- [11] CHORUS Collaboration, A. Kayis-Topaksu, et al., *Phys. Lett. B* 527 (2002) 173.
- [12] CHORUS Collaboration, E. Eskut, et al., *Nucl. Instrum. Methods A* 401 (1997) 7.
- [13] S. Aoki, et al., *Nucl. Instrum. Methods A* 447 (2000) 361.
- [14] T. Nakano, Ph.D. Thesis, Nagoya University, 1997.
- [15] DONUT Collaboration, K. Kodama, et al., *Phys. Lett. B* 504 (2001) 218.
- [16] A.M. Güler, Ph.D. Thesis, Middle East Technical University, Ankara, 2000.
- [17] B. Van de Vyver, Ph.D. Thesis, Vrije Universiteit Brussel, 2002, CERN-THESIS-2002-024.
- [18] GEANT 3.21, CERN program library long writeup W5013.
- [19] P. Zucchelli, Ph.D. Thesis, Università di Ferrara, 1995.
- [20] G. Ingelman, LEPTO version 6.1: the Lund Monte Carlo for deep inelastic lepton–nucleon scattering, in: W. Buchmüller, G. Ingelman (Eds.), *Workshop on Physics at HERA*, 1992, pp. 1366–1394.
- [21] T. Sjöstrand, *Comput. Phys. Commun.* 82 (1994) 74.
- [22] O. Melzer, Ph.D. Thesis, Universiteit van Amsterdam, 2001.
- [23] P. Migliozi, G. D’Ambrosio, G. Miele, P. Santorelli, *Phys. Lett. B* 462 (1999) 217.
- [24] C.G. Wohl, The sad state of charmed-particle branching fractions, unpublished, Particle Data Group note, 2002.